https://doi.org/10.5194/egusphere-2025-4430
Preprint. Discussion started: 8 December 2025

Temperature Dependence of Ice Crystal Size in Tibetan Ice Core

Zhengqiang He[1,2], Baiqing Xu[1]

[1]Key Laboratory of Tibetan Environment Changes and Land Surface Processes, Institute of Tibetan Plateau Research, Chinese Academy of Sciences, Beijing 100101, China
[2]University of Chinese Academy of Science, Beijing 100049, China

Correspondence to: Baiqing Xu (baiqing@itpcas.ac.cn)

Abstract. The ice crystal size in ice core can not only reflect the glacial strain process but also be connected to climate change. However, the process of ice crystal size variation along ice core in mountain glacier remains largely unexplored. Here, we continuously measured the ice grain areas along two deep ice cores drilled from the Tibetan Plateau, and found that the two ice cores exhibit vertical grain area differentiation at the hundred-meter scale, analogous to polar ice-core profiles, relatively higher temperatures significantly accelerate grain growth and result in larger grain areas. Refreezing under warm conditions gives rise to abrupt increases in grain area within melt-refrozen layers, whereas impurities result in abrupt decreases in grain area within cloudy bands. Together, these two factors drive centimeter-scale fluctuations in grain area. Even so, we also found that grain area exhibits a significant correlation with $\delta^{18}O$ in ice layers where Rotation Recrystallization (RRX)-induced refinement is negligible, indicating that the ice crystal size of mountain glaciers ice core can retain temperature signals.

1 Introduction

As a critical component of the Earth's climate system, glaciers not only dynamically feedback to global climate patterns but also enable systematic reconstruction of past glacial evolution and climatic history through the physical and chemical records in ice cores. Notably, ice crystal size in ice cores can reflect both glacial strain processes (Gow and Williamson, 1976; Alley et al., 1986a, b; Hellmann et al., 2020) and be connected to climate change (Svensson et al., 2003; Durand et al., 2007; Fitzpatrick et al., 2014).

After decades of research, the polar ice core "three-stage model" is widely adopted to characterize ice crystal size variation profiles and clarify grain growth/recrystallization mechanisms (Alley et al., 1986a, b; Faria et al., 2014a). However, high-resolution studies have revealed limitations in this classic model—especially for short-scale ice crystal evolution and analysis of multiple factors, stimulating ongoing refinements and scientific debates (Kipfstuhl et al., 2006, 2009; Weikusat et al., 2009; Faria et al., 2014b; Kerch, 2016).

The complexity of ice crystal evolution is amplified in mid-latitude mountain glaciers, which typically feature higher temperatures, greater accumulation rates, and faster flow velocities. These characteristics accelerate grain variation and induce significant centimeter-scale fluctuations in microstructures (Kerch, 2016; Hellmann et al., 2020).

https://doi.org/10.5194/egusphere-2025-4430
Preprint. Discussion started: 8 December 2025

As typical mid-latitude mountain glaciers, Tibetan Plateau glaciers have shown enhanced to climate sensitivity in recent decades (Yao et al., 2012). Regional climatic and topographic heterogeneities across these glaciers drive distinct ice formation processes and and divergent microstructural characteristics. However systematic study on ice crystal evolution, recrystallization and responses to temperature remains notably scarce (Zhang et al., 1993; Li et al., 2017).

This study is thus based on two mountain glacier ice cores drilled in the Tibetan Plateau: Animaqing (ANMQ) and Bugyai Kangri (BJGR). Using a Microstructure Mapping system, we successfully obtained continuous longitudinal microstructure images spanning from the firn to the base of both ice cores and present the first continuous ice grain area profiles for mountain glacier ice cores. This dataset compensates for the centimeter-scale microstructural variations missed by traditional discrete sampling,

This study aims to address three key questions: (1) What are the vertical variations in ice crystal size and recrystallization mechanisms in mountain glacier ice cores under high-temperature conditions? (2) How do impurities and refreezing processes affect centimeter-scale fluctuations? (3) Can ice crystal size in mountain ice cores retain information about climate change? By providing new microscopic evidence, this study advances the fundamental understanding of ice crystal size variation and recrystallization mechanisms in mid-latitude mountain glacier ice cores and offers a new perspective for exploring the responses of Tibetan Plateau mountain glaciers to climate change.

2 Samples and methods

The ANMQ deep ice core (169.5 m long) was drilled at the summit of Weigeledangxiong Glacier (Mount Animaqing; 99.45°E, 34.81°N, 5750 m a.s.l.) in November 2020, whereas The BJGR deep ice core (77.6 m long) was drilled at the summit of the Poge Glacier (southern slope of Mount Bugyai Kangri; 94.70°E, 31.82°N, 6180 m a.s.l.) in November 2022 (Fig. 1a). Both regions are mainly influenced by the East Asian Monsoon. The annual precipitation and temperature near the snow line are 600–700 mm and −6 ℃ for BJGR, and 700–900 mm and −9.4 ℃ for ANMQ respectively (Liu et al., 2016; Jiang et al., 2018). After drilling, borehole temperatures were measured (Fig. 1b), and the ice cores were transported to a cold laboratory for storage at −20 ℃.

These ice cores were then continuously sectioned along their longitudinal axes (Fig. 2a). A total of 560 slices (sampling rate: 71%) were obtained from 22.30 m to the base of the BJGR core, and 1890 slices (sampling rate: 91%) were collected from 14.94 m to the base of the ANMQ core. Each slice measures approximately 6–10 cm in length, ~4.5 cm in width, and ~7 mm in thickness. The surface of each ice slice was trimmed flat using a Leica SM2000R slicer and then sublimated at ~ −20℃ for approximately 15 hours, until the surface became smooth and exhibited clearly visible grain boundaries.

Finally, the ice slice was placed on a black background, and microstructural images were acquired using a Microstructure Mapping system, which followed the protocol described in previous studies (Fig. 2b, Kipfstuhl, 2006; Fegyveresi, 2015). The image resolution is ~8 μm/pixel. Each panoramic image of the slice was automatically and seamlessly stitched from 5 consecutive photos using the Photomerge function in Photoshop software(Fig. 2c). After that, irregular image edges were

https://doi.org/10.5194/egusphere-2025-4430
Preprint. Discussion started: 8 December 2025

cropped, and interfering factors (e.g., scratches and cracks) were manually removed. Binary segmentation was performed with the U-Net neural network (Ronneberger et al., 2015), and grain-boundary maps were generated using ImageJ software with the MorphoLibJ plugin (Fig. 2a, 2b, and 2c); Legland et al., 2016). After scale calibration, data on grain and bubble areas, position, and shape were extracted. These results were then correlated with depth data for statistical analysis .

3 Results and discussion

3.1 Grain area profile and recrystallization mechanism

Fresh snow crystals (~1 mm²) evolve continuously with increasing depth and time, adapting to temperature and stress conditions via deformation and recrystallization. This evolutionary process can be characterized by microstructural images and ice crystal size statistical data. In this study, we observed that the vertical profiles of grain area, porosity, and density in the ANMQ and BJGR ice cores exhibit hundred-meter-scale differentiation patterns analogous to polar ice cores profiles (Fig. 4, and A1; Faria et al., 2014a). Based on this observation, we classified their grain area profiles into distinct layers and analyzed the dominant recrystallization mechanisms. These efforts aim to establish a foundational understanding of ice crystal size variation in Tibetan Plateau mountain glacier ice cores.

3.1.1 Firn layer (<35 m)

In this layer, as depth increases, numerous irregularly shaped unclosed pores are progressively compressed, leading to an increase in density. Both ice cores reached the critical density of 0.830 g/cm³ for pore closure at ~35 m depth (Fig. A2b; Dadic et al., 2019). The average grain area is small and increases slowly (ANMQ: 2–5 mm²; BJGR: 1–3 mm²). Grains >1 mm² and those ≤ 1 mm² each constitute approximately 50% of the total, while grains >5 mm² account for ~10% (Fig. 4).

3.1.2 Growth layer (35–45 m)

In this layer, pores become isolated from the free atmosphere, with ~10% of the original air volume eventually trapped as enclosed bubbles and gradually compressed into ellipsoidal shapes (Schaller et al., 2017). The firn transforms into ice, and the average grain area increases rapidly with fluctuations (ANMQ: 10–20 mm²; BJGR: 5–10 mm²). The ice crystal size becomes heterogeneous, and grain boundaries begin to curve.

In the firn and growth layers (which are typically classified as a single layer in polar studies), the average grain area increases while the grain number decreases. The average grain area and proportion of grains >5 mm² increase, whereas the small-grain average grain area decreases and their proportion increases slightly (Fig. 4). Additionally, typical "foam" textures formed by Normal Grain Growth (NGG) are observable in microstructure images (Fig. 3d) (Svensson et al., 2005). This indicates that grain growth primarily results from larger grains consuming smaller ones.

https://doi.org/10.5194/egusphere-2025-4430
Preprint. Discussion started: 8 December 2025

These observations indicate that ice crystal size in these two layers is significantly influenced by NGG, which is primarily regulated by temperature (Gow, 1969). Generally, higher temperatures tend to promote the formation of larger ice crystals (Cuffey & Paterson, 2010), such that the grain area of the ANMQ ice core with higher temperature (Fig. 1b) is larger than that of the BJGR.

3.1.3 Stable layer (ANMQ: 45–140 m; BJGR: 45–73 m)

In this layer, the average grain area stabilizes and decline to ~5 mm². Both the average grain area and proportions of grains >5 mm² gradually decrease, while the small-grain proportions and total grain number increase (Fig. 4, and A2a). In microstructure images, Abundant subgrain boundaries are observed (Fig. 3e). This indicates that the average grain area decline primarily results from large grains splitting into smaller ones.

These observations indicate that the stable layer is mainly influenced by RRX. Under stress conditions, subgrain boundaries form inside grains and gradually develop into grain boundaries, splitting large grains into smaller ones (Weikusat et al., 2009; 2017). This stress-induced grain refinement restricts the growth of large grains (Duval and Castelnau, 1995). However, average grain area in deeper ANMQ layers remains larger than that in the shallow BJGR,layers, despite stronger vertical pressures on the former, which suggest that higher temperatures have enhanced grain growth, resulting in a larger equilibrium grain area.

3.1.4 Mutation layer (ANMQ: 140–169. 5 m; BJGR: 73–77.6 m)

This layer is located at the bottom of the ice core. The average grain area increases rapidly with drastic fluctuations. The growth rate of grains > 5 mm² is approximately 10 times higher than that in the growth layer (Fig. A3), with their proportion rising rapidly(Fig. 4). In microstructure images, large grains exhibit interlocked structures, accompanied by the connection between subgrain boundaries and highly curved grain boundaries (Fig. 3f).

These observations are consistent with rapid grain boundary migration dominated by Strain-Induced Boundary Migration (SIBM), which tends to occur when ice temperatures are above -10 °C (Duval and Castelnau, 1995; Faria et al., 2014b). The basal temperatures of both ice cores satisfy this criterion. Notably, in ANMQ ice core, grains grow rapidly below 150 m depths, accompanied by oversized grains and a 5-meter-thick basal pure ice layer. This pattern is likely linked to the temperature transition at 150 m, where the temperature shifts from decreasing to increasing. These findings indicate that basal temperatures also influence ice crystal size in the mutation layer.

3.2 Temperature, refreezing processes, and impurities influences

The above results indicate that temperature influences ice crystal size by regulating recrystallization across all layers. Furthermore, temperature differences have also contributed to variations in ice formation processes between the two ice cores.

https://doi.org/10.5194/egusphere-2025-4430
Preprint. Discussion started: 8 December 2025

The BJGR ice core, with relatively lower temperatures, exhibits lower firn density and smaller ice crystal sizes, embodying typical characteristics of Cold-type Ice Genesis (i.e., ice formation without meltwater involvement; Cuffey and Paterson, 2010). Before pore closure, the higher surface energy of smaller grains tends to drive sublimation, some water molecules condense on larger grains with lower surface energy, while others diffuse into the free atmosphere. After pore closure, large grains grow rapidly by consuming smaller ones.

The ANMQ ice core, with relatively higher temperatures and surface temperature approaching 0 °C, contains numerous centimeter-scale melt-refrozen ice layers in its firn layer(Fig. 5a), embodying typical Warm-type Ice Genesis (i.e., ice formation involving meltwater percolation; Cuffey and Paterson, 2010). Meltwater percolation and liquid-mediated recrystallization drive accelerated densification and larger ice crystal sizes, with both the average grain area and growth rate exceeding those of BJGR. Additionally, these high-temperature-induced melt-refrozen ice layers—also observed in some sections of the BJGR firn layer—lead to abrupt increases in average grain area and serve as a critical factor driving centimeter-scale average grain area fluctuations.

When comparing with other mountain glacier ice cores, the firn layer temperatures of these two ice cores are significantly higher (> -6 °C) and follow a thermal gradient: ANMQ > BJGR > Guliya ≈ Alpin KCC. This gradient aligns with the ranking of average grain area and growth rate (Kerch, 2016; Li et al., 2017), further confirming temperature as the dominant factor governing grain growth in these mountain glaciers.

We also observed numerous cloudy bands (mm to cm scale) in both ice cores (Fig. 5b). Within these layers, abundant small grains (typically < 2 mm^2)—form multiple small-grain walls, lead to abrupt decreases in average grain area. Generally, the total thickness of cloudy bands is < 20 cm per meter (Fig. A4). However, in the ANMQ ice core, there is a dense zone of cloudy bands at 120–140 m depth (total thickness up to 90 cm), which shows a strong negative correlation with average grain area ($r = -0.715$, $p < 0.01$; Fig. A4). A less prominent dense zone of cloudy bands is also observed in the BJGR ice core at 66–75 m depth.

Polar ice core research shows ice crystal sizes in cloudy bands are typically smaller and negatively correlated with impurity concentration (Alley and Woods 1996; Svensson et al., 2005). This is because impurities inhibit grain boundary migration by reducing migration rates and "pinning" grain boundaries, thereby restricting grain growth (Weiss et al., 2002; Durand et al., 2006; Faria et al., 2010; Eichler et al., 2019; Stollet al., 2021). In these two ice cores, impurity-induced grain growth restriction is another critical factor driving centimeter-scale average grain area fluctuations.

3.3 The link between ice crystal size and climate change

Ice crystal size is significantly influenced by temperature, which is modulated by air temperature. Theoretically, ice crystal size can preserve climate change information. Studies on polar ice cores (e.g., NGRIP, EDC, WAIS) indicate that ice crystal size is typically linked to climate history: average grain area usually correlates with other climate proxies (e.g., $\delta^{18}O$), and its abrupt changes often correspond to cold-warm transitions or paleoclimatic cold/hot events (Svensson et al., 2003; Durand et

https://doi.org/10.5194/egusphere-2025-4430
Preprint. Discussion started: 8 December 2025

al., 2007; Fitzpatrick et al., 2014). However, the ice crystal size of these two ice cores is influenced by high temperatures, melt-refrozen ice layers, and impurities—can it still retain climate information amid these multiple influences?

In studies of Tibetan Plateau ice cores, $\delta^{18}O$ have been widely used to reconstruct climate change history (Thompson et al., 1997). We compared the average grain area with $\delta^{18}O$ of thes two ice cores and found that, at 45–51 m depth in both ice cores, their average grain area and $\delta^{18}O$ show comparable fluctuation: the BJGR ice core show a significant negative correlation ($r = -0.286$, $p < 0.01$; Fig. 6a, 6b), while the correlation is insignificant in the ANMQ due to strong refreezing interference.

Additionally, average grain area and $\delta^{18}O$ also show comparable fluctuation in the dense zone of cloudy bands: the ANMQ ice core shows a significant correlation ($r = 0.205$, $p < 0.01$; Fig. 6c, 6d), while the correlation is insignificant in the BJGR due to lower cloudy bands density. The low $\delta^{18}O$ values in the dense zone of cloudy bands indicate cold climatic periods, which aligns with previous studies demonstrating that densified cloudy bands and elevated dust concentrations typically occur during cold periods (Ram et al., 1997; Mahowald et al., 1999; Overpeck et al., 1996).

At 45–51 m depth, RRX-induced grain refinement is minimal since low vertical pressures, and grain growth dominated by temperature-dependent NGG. In the dense zone of cloudy bands, low temperatures and impurity-induced restriction result in smaller ice crystal sizes and limited strain accumulation, thereby inhibiting RRX-induced grain refinement. This allows ice crystal sizes to retain temperature-sensitive signals in both intervals. This lays the groundwork for further exploring the connections between the physical characteristics—such as bubble number density—of mountain glacier ice cores and climate change (Spencer et al., 2016; Fegyveresi et al., 2016; Lipenkov, 2018).

4 Conclusions

This study presents the first continuous profiles of ice grain area spanning from the firn to the base of two deep mountain glacier ice cores from the Tibetan Plateau, revealing vertical differentiation in grain area at the hundred-meter scale, analogous to polar ice core profiles. Temperature is the key factor influencing ice crystal evolution across all depth intervals. Relatively higher temperatures significantly enhance grain growth, thus resulting in a larger equilibrium grain area. Refreezing under warm conditions gives rise to abrupt increases in grain area within melt-refrozen layers, whereas impurities result in abrupt decreases in grain area within cloudy bands. Together, these two factors drive centimeter-scale fluctuations in grain area. Notably, in layers where RRX-induced refinement is negligible, grain area exhibits a significant correlation with $\delta^{18}O$, indicating that ice crystal size in mountain glacier ice cores can still retain temperature signals despite multiple influencing factors.

https://doi.org/10.5194/egusphere-2025-4430
Preprint. Discussion started: 8 December 2025

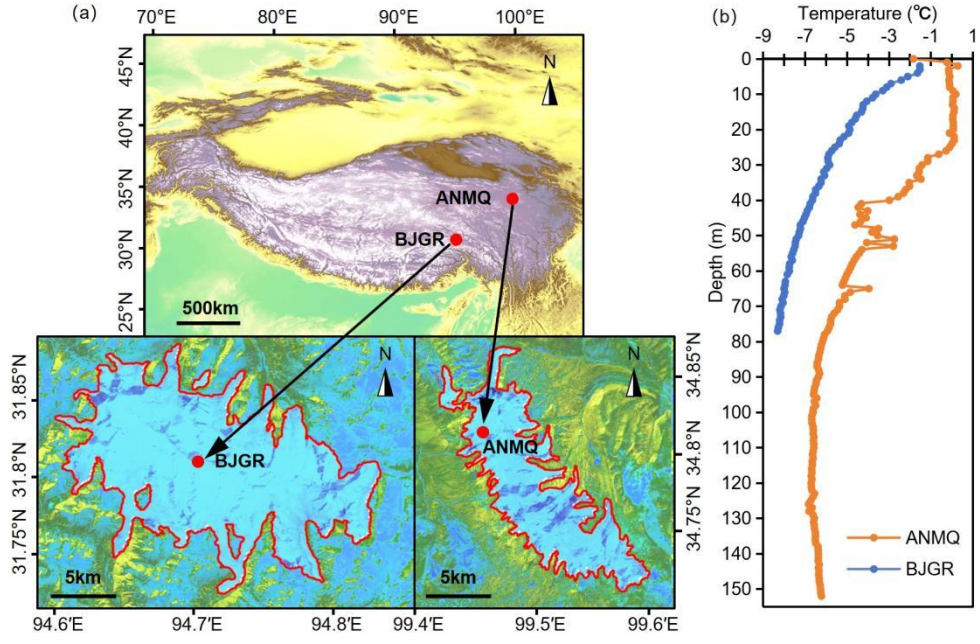

Figure 1. (a) Drilling sites of the ANMQ and BJGR ice cores; (b) Borehole temperatures, measured using a 150 m resistance temperature sensor cable with an accuracy of ±0.02 °C. Temperatures below 150 m in the ANMQ ice core were not measured.

https://doi.org/10.5194/egusphere-2025-4430
Preprint. Discussion started: 8 December 2025

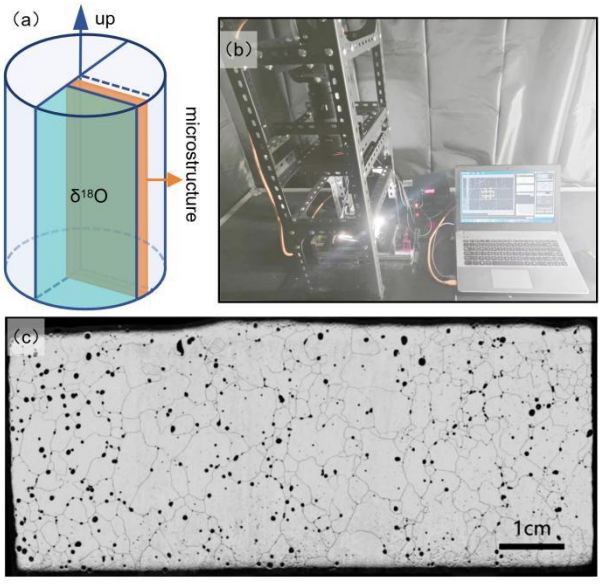

Figure 2. (a) Schematic diagram of ice slice cutting; the orange section represents a slice with approximate dimensions: 10 × 4.5 × 0.7 cm; (b) Photograph of the microstructure mapping system. The system comprises an imaging module (equipped with a Canon EOS 5D Mark IV camera and an 180 mm macro lens), an illumination module (including a vertical coaxial light source and a light controller), and a manual X-axis translation stage. Photo-shooting parameters, focusing, and image capture were controlled via Canon Camera Connect software; (c) Seamlessly stitched panoramic image of a slice, generated from 5 consecutive photos.

https://doi.org/10.5194/egusphere-2025-4430
Preprint. Discussion started: 8 December 2025

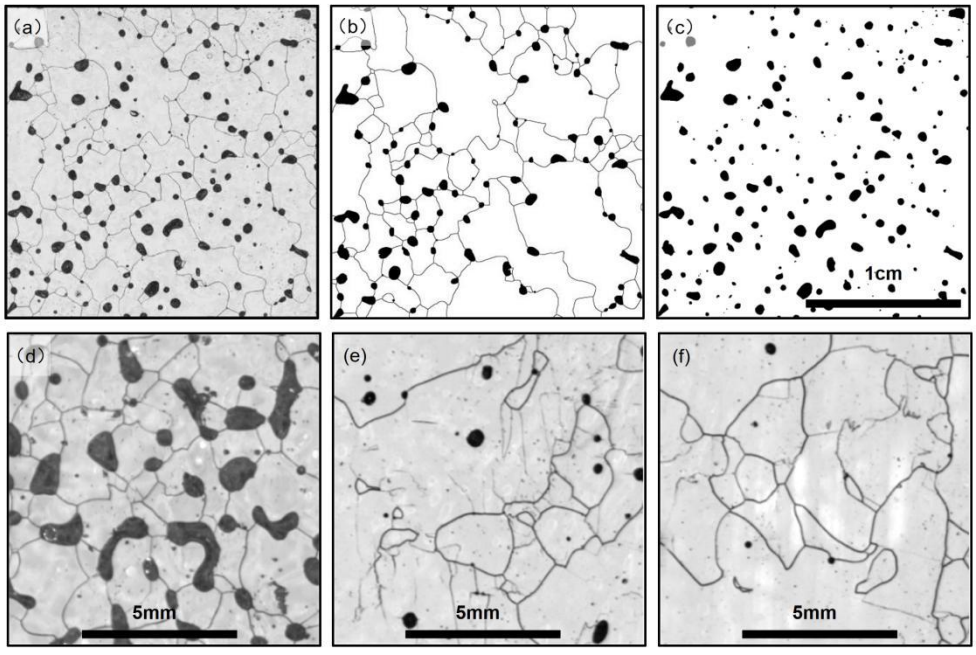

Figure 3. Microstructure images and image processing procedures: (a) Original microstructural image (ANMQ-T49B15); (b) Grain boundary map; (c) Pore/bubble map; (d)–(f) Microstructural images of the BJGR ice core: straight grain boundaries and triple junctions in the firn layer; abundant subgrain boundaries in the stable layer; subgrain boundaries and highly curved grain boundaries in the mutation layer.

https://doi.org/10.5194/egusphere-2025-4430
Preprint. Discussion started: 8 December 2025

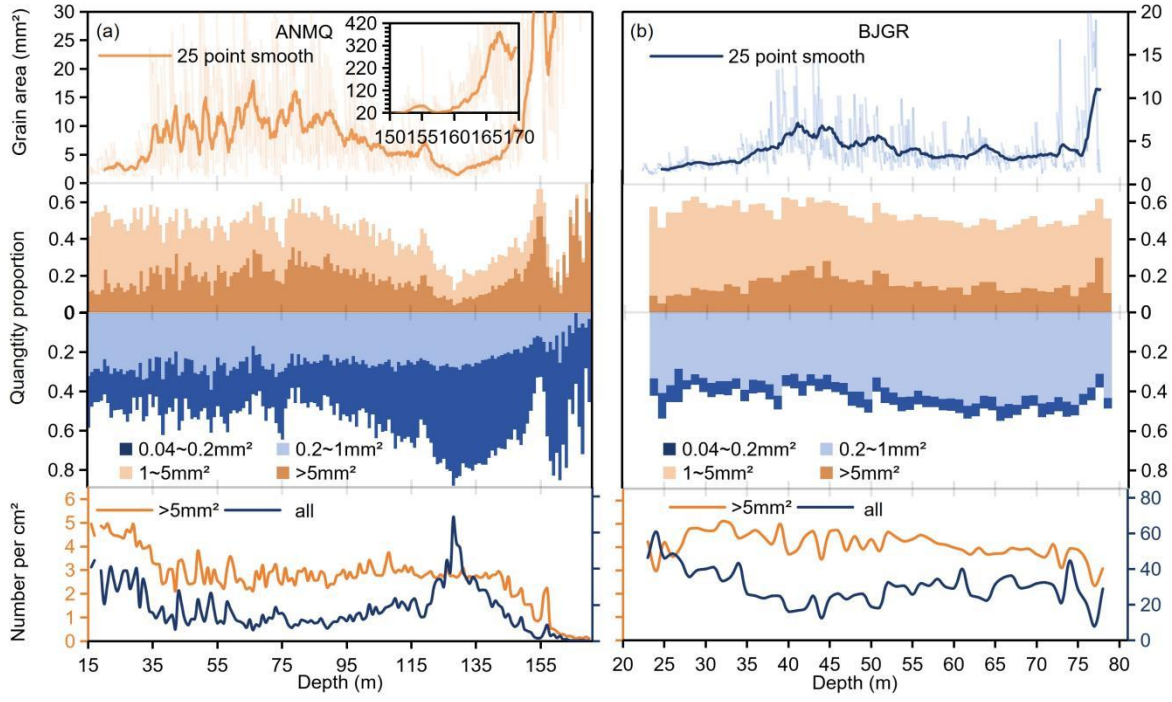

Figure 4. Profiles of average grain area and proportion of grain quantities across different size ranges: (a) For the ANMQ ice core; the inset depicts rapid grain growth, with the grain area reaching ~400 mm² near the base of the core; (b) For the BJGR ice core. Thin lines represent 2 cm resolution data, while bold lines represent 25 point smoothed data. The number of grains in different size grades was statistically analyzed on a per meter basis.

https://doi.org/10.5194/egusphere-2025-4430
Preprint. Discussion started: 8 December 2025

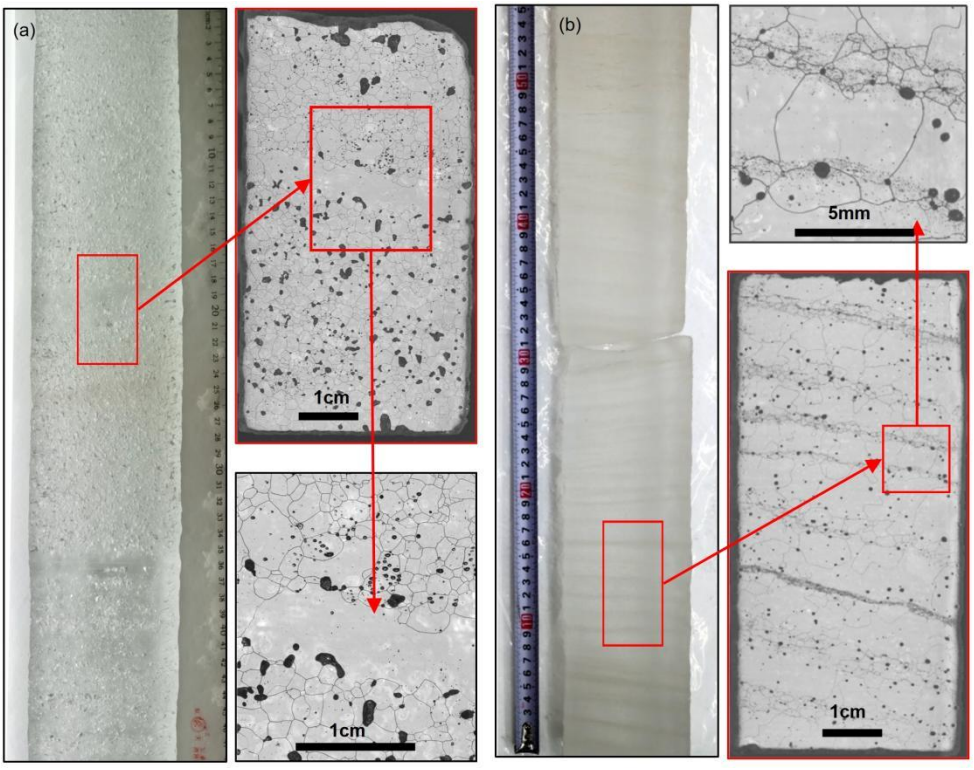

Figure 5. Illustrations of centimeter-scale fluctuations in the ANMQ ice core: (a) Photograph of a melt-refrozen layer in the firn layer, with a magnified inset showing abrupt enlargement of grain area; (b) Photograph of a dense zone of cloudy bands, with a magnified inset displaying clustering of small grains.

https://doi.org/10.5194/egusphere-2025-4430
Preprint. Discussion started: 8 December 2025

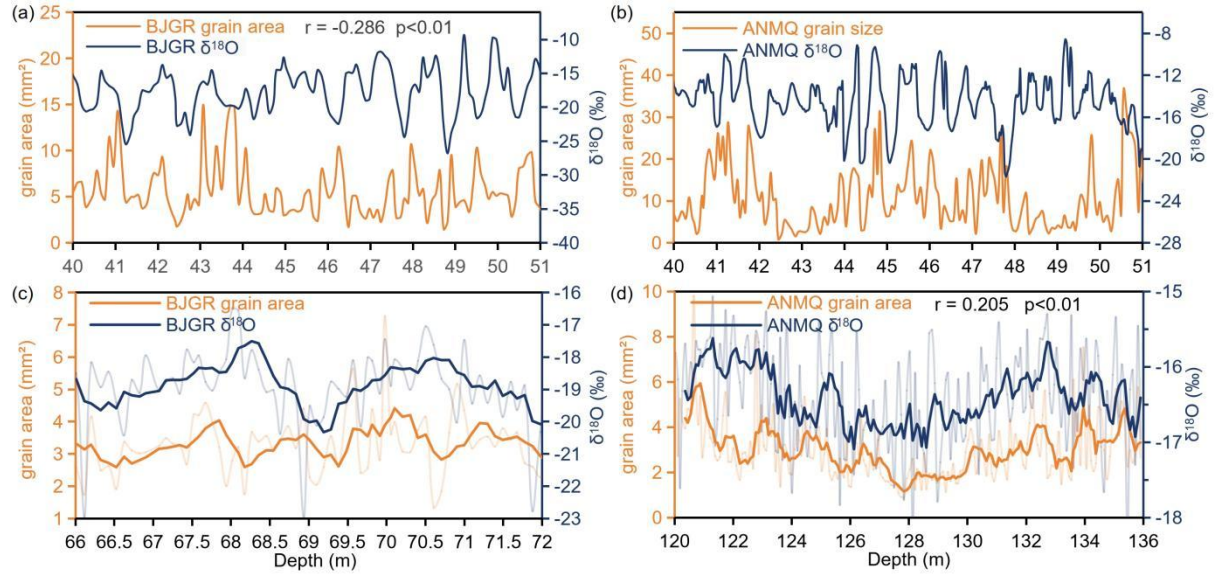

Figure 6. Comparison between average grain area and δ¹⁸O values: (a) and (b) in the 40–51 m interval show inverse fluctuations because the "amount effect" results in lower δ¹⁸O values in summer and higher values in winter (Yang, 2024, Unpublished doctoral dissertation). (c) and (d) show similar fluctuations in the dense zones of cloudy bands. The thin lines represent 2 cm resolution data, and the bold lines represent 5 point smoothed data.

https://doi.org/10.5194/egusphere-2025-4430
Preprint. Discussion started: 8 December 2025

Appendix A

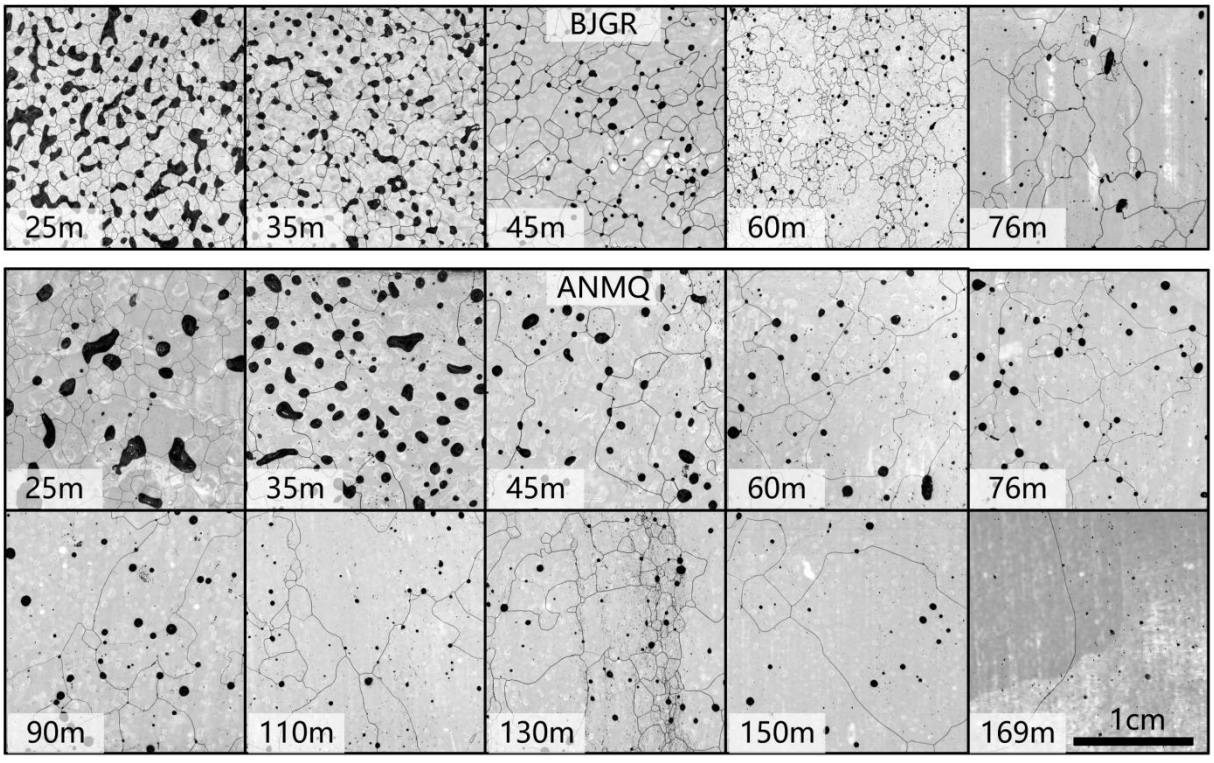

Figure A1. Exemplary microstructure images of BJGR and ANMQ ice cores; Microstructure images at different depths are selected, showing significant variations in grain area and bubbles.

https://doi.org/10.5194/egusphere-2025-4430
Preprint. Discussion started: 8 December 2025

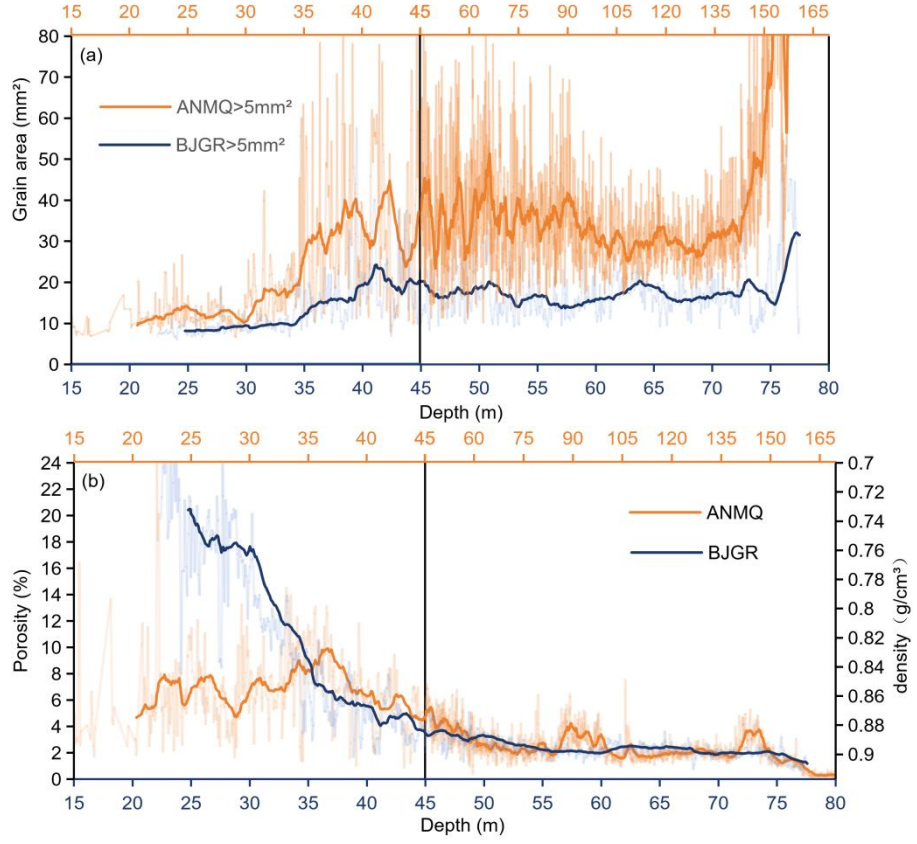

Figure A2. (a) Average area of grains >5mm² profiles of ANMQ and BJGR ice cores. The average area of all grains is significantly correlated with the average area of grains >5mm² (ANMQ: r=0. 847, p<0. 01; BJGR: r=0. 909, p<0. 01); (b) The porosity and density profiles of ANMQ and BJGR ice cores; The thin lines represent original data, the bold lines represent the 25 point smooth.

The ice core density was deduced using the formul: density = (1 − porosity) × 0.917 g/cm³ (Kerch, 2016). Due to the fragility of loose firn slice samples in the upper part of the ANMQ ice core, combined with the retention of many melt-refrozen ice layer samples, this sampling error caused abnormally high density values and a downward trend above 35 m in the ANMQ ice core. The section below 45 m of the ANMQ core is compressed onto a reduced scale.

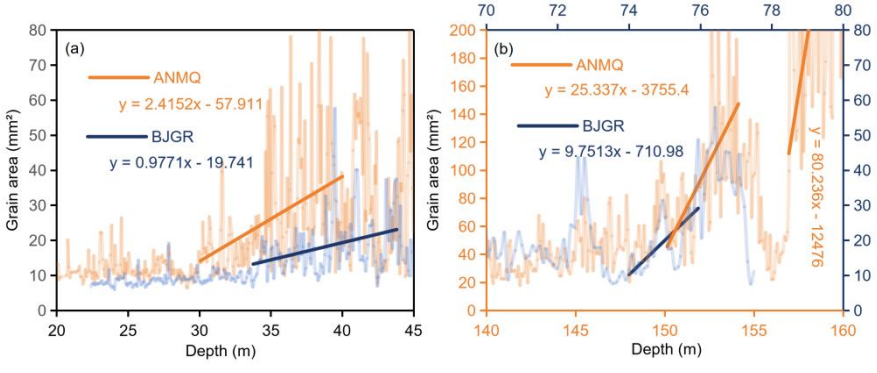

https://doi.org/10.5194/egusphere-2025-4430
Preprint. Discussion started: 8 December 2025

Figure A3. Growth rate of grains > 5 mm²: (a) Growth layer; (b) Mutation layer; The thin lines represent 2 cm resolution data, the bold lines represent linear fitting results.

Below 156 m depth in the ANMQ ice core, the growth rate of grains >5 mm² reaches up to 80 mm²/m At the base, grain areas exceed 3000 mm², with grain boundaries extending beyond ice slice edges. Concurrently, impurity layers vanish, and the ice core approximates transparent pure ice. We infers that the grains at this depth underwent intense refreezing: excessive temperatures caused extensive melting, and prolonged high temperatures induced repeated freeze-thaw cycles, ultimately generating exceptionally large grains. High-temperature-induced melt-refrozen ice layers are a primary driver of the abrupt grain area increase at the ANMQ core base, implying the glacier experienced historical high-temperature events.

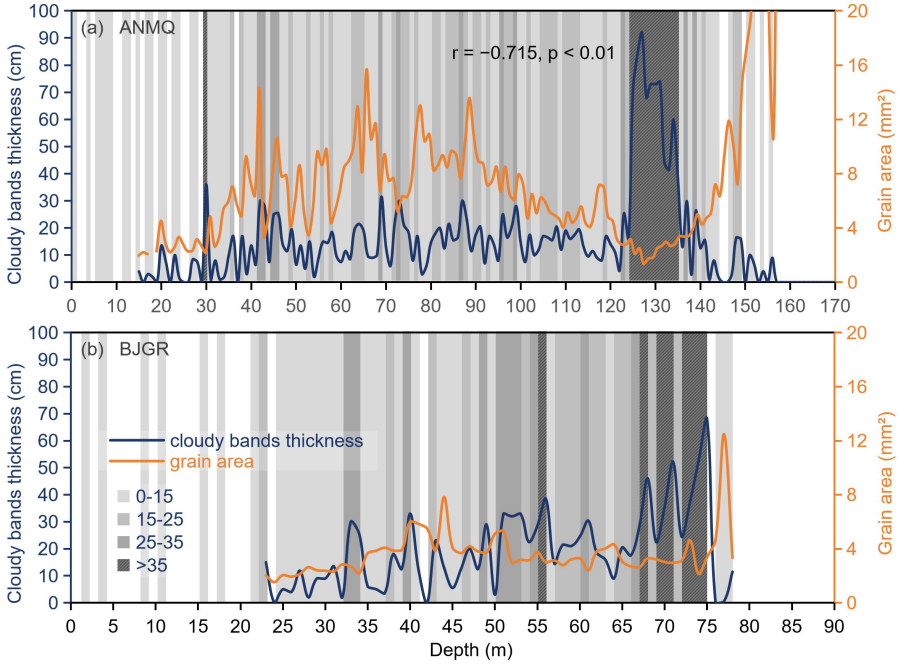

Figure A4. Variation sequences of cloudy bands thickness and average grain area: (a) ANMQ; (b) BJGR; Background colors also indicate the thickness of cloudy bands.

https://doi.org/10.5194/egusphere-2025-4430
Preprint. Discussion started: 8 December 2025

Data availability. Microstructure images and raw grain parameter data are available upon request.

Author contributions. Zhengqiang He designed the study, conducted field sampling and laboratory experiments, analyzed the data, and drafted the manuscript; Baiqing Xu supervised the research, revised the manuscript critically, and secured funding.

Competing interests. The contact author has declared that neither they nor their co-authors have any competing interests.

Acknowledgments. We thank all personnel involved in the drilling of the ANMQ and BJGR ice cores and the associated experiments. Special appreciation is extended to Bo Fang, Siyv Lu, Xiaoxi Zhu, and Jiajia Wang for their valuable assistance and insightful suggestions.

Financial support. This research was supported by Excellent Research Group Program for Tibetan Plateau Earth System (No. 42588201).

References

Alley, R. B., Perepezko, J. H., & Bentley, C. R. (1986a). Grain growth in polar ice: I. Theory. Journal of Glaciology, 32(112), 415-424.

Alley, R. B., Perepezko, J. H., & Bentley, C. R. (1986b). Grain growth in polar ice: II. Application. Journal of Glaciology, 32(112), 425-433.

Alley, R. B., & Woods, G. A. (1996). impurity influence on normal grain growth in the GISP2 ice core, Greenland. Journal of Glaciology, 42(141), 255-260.

Cuffey, K. M., & Paterson, W. S. B. (2010). The physics of glaciers (4th ed.). Academic Press.

Dadic, R., Schneebeli, M., Wiese, M., Bertler, N. A. N., Salamatin, A. N., Theile, T. C., . & Lipenkov, V. Y. (2019). Temperature-driven bubble migration as proxy for internal bubble pressures and bubble traping function in ice cores. Journal of Geophysical Research: Atmospheres, 124(17-18), 10264-10282.

Duval, P., & Castelnau, O. (1995). Dynamic recrystallization of ice in polar ice sheets. Le Journal de Physique IV, 5(C3), C3-197.

Durand, G., Weiss, J., Lipenkov, V., Barnola, J. M., Krinner, G., Parrenin, F., . & Bigler, M. (2006). Effect of impurities on grain growth in cold ice sheets. Journal of Geophysical Research: Earth Surface, 111(F1).

Durand, G., Gillet-Chaulet, F., Svensson, A., Gagliardini, O., Kipfstuhl, S., Meyssonnier, J., . & Dahl-Jensen, D. (2007). Change in ice rheology during climate variations–implications for ice flow modelling and dating of the EPICA Dome C core. Climate of the Past, 3(1), 155-167.

Eichler, J., Weikusat, C., Wegner, A., Twarloh, B., Behrens, M., Fischer, H., ... & Weikusat, I. (2019). impurity analysis and microstructure along the climatic transition from MIS 6 into 5e in the EDML ice core using cryo-Raman microscopy. Frontiers in Earth Science, 7, 20.

Faria, S. H., Freitag, J., & Kipfstuhl, S. (2010). Polar ice structure and the integrity of ice-core paleoclimate records. Quaternary Science Reviews, 29(1-2), 338-351.

https://doi.org/10.5194/egusphere-2025-4430
Preprint. Discussion started: 8 December 2025

Faria, S. H., Weikusat, I., & Azuma, N. (2014a). The microstructure of polar ice. Part I: Highlights from ice core research. Journal of Structural Geology, 61, 2-20.

Faria, S. H., Weikusat, I., & Azuma, N. (2014b). The microstructure of polar ice. Part II: State of the art. Journal of Structural Geology, 61, 21-49.

Fegyveresi, J. M. (2015). Physical properties of the West Antarctic Ice Sheet (WAIS) Divide deep core: Development, evolution, and interpretation. The Pennsylvania State University.

Fegyveresi, J. M., Alley, R. B., Fitzpatrick, J. J., Cuffey, K. M., McConnell, J. R., Voigt, D. E., ... & Stevens, N. T. (2016). Five millennia of surface temperatures and ice core bubble characteristics from the WAIS Divide deep core, West Antarctica. Paleoceanography, 31(3), 416-433.

Fitzpatrick, J. J., Voigt, D. E., Fegyveresi, J. M., Stevens, N. T., Spencer, M. K., Cole-Dai, J., . & McCONNELL, J. R. (2014). Physical properties of the WAIS Divide ice core. Journal of Glaciology, 60(224), 1181-1198.

Gow, A. J. (1969). On the rates of growth of grains and crystals in South Polar firn. Journal of Glaciology, 8(53), 241-252.

Gow, A. J., & Williamson, T. (1976). Rheological implications of the internal structure and crystal fabrics of the West Antarctic ice sheet as revealed by deep core drilling at Byrd Station. Geological Society of America Bulletin, 87(12), 1665-1677.

Hellmann, S., Kerch, J., Weikusat, I., Bauder, A., Grab, M., Jouvet, G., . & Maurer, H. (2020). Crystallographic analysis of temperate ice on Rhonegletscher, Swiss Alps. The Cryosphere Discussions, 2020, 1-22.

Hörhold, M. W., Laepple, T., Freitag, J., Bigler, M., Fischer, H., & Kipfstuhl, S. (2012). On the impact of impurities on the densification of polar firn. Earth and Planetary Science Letters, 325, 93-99.

Jiang, Z. L., Liu, S. Y., Guo, W. Q., Li, J., Long, S. C., Wang, X., & Wu, K. P. (2018). Recent changes in the surface elevation of typical glaciers in the Animaqing Mountains in the Yellow River source area [J]. Journal of Glaciology and Geocryology, 40(2), 231-237.

Kerch, J. K. (2016). Crystal - orientation fabric variations on the cm - scale in cold Alpine ice: Interaction with paleo - climate proxies under deformation and implications for the interpretation of seismic velocities [Doctoral dissertation].

Kipfstuhl, S., Hamann, I., Lambrecht, A., Freitag, J., Faria, S. H., Grigoriev, D., & Azuma, N. (2006). Microstructure mapping: a new method for imaging deformation - induced microstructural features of ice on the grain scale. Journal of Glaciology, 52(178), 398-406.

Kipfstuhl, S., Faria, S. H., Azuma, N., Freitag, J., Hamann, I., Kaufmann, P., … & Wilhelms, F. (2009). Evidence of dynamic recrystallization in polar firn. Journal of Geophysical Research: Solid Earth, 114(B5), B05204.

Legland, D., Arganda - Carreras, I., & Andrey, P. (2016). MorphoLibJ: integrated library and plugins for mathematical morphology with ImageJ. Bioinformatics, 32(22), 3532 - 3534.

Llorens, M. G., Griera, A., Steinbach, F., Bons, P. D., Gomez-Rivas, E., Jansen, D., ... & Weikusat, I. (2017). Dynamic recrystallization during deformation of polycrystalline ice: insights from numerical simulations. Philosophical Transactions of the Royal Society A: Mathematical, Physical and Engineering Sciences, 375(2086), 20150346.

https://doi.org/10.5194/egusphere-2025-4430
Preprint. Discussion started: 8 December 2025

Li, Y., Kipfstuhl, S., & Huang, M. (2017). Ice microstructure and fabric of Guliya ice cap in Tibetan plateau, and comparisons with vostok3G-1, EPICA DML, and north GRIP. Crystals, 7(4), 97.

Lipenkov, V. Y. . (2018). How air bubbles form in polar ice. Earth's Cryosphere, 22(2), 16-28.

Liu, Q., Guo, W. Q., Nie, Y., Liu, S. Y., & Xu, J. L. (2016). Recent glacier and glacial lake changes and their interactions in the Bugyai Kangri, southeast Tibet. Annals of Glaciology, 57(71), 61-69.

Mahowald, N., Kohfeld, K., Hansson, M., Balkanski, Y., Harrison, S. P., Prentice, I. C., . & Rodhe, H. (1999). Dust sources and deposition during the last glacial maximum and current climate: A comparison of model results with paleodata from ice cores and marine sediments. Journal of Geophysical Research: Atmospheres, 104(D13), 15895-15916.

Overpeck, J., Rind, D., Lacis, A., & Healy, R. (1996). Possible role of dust-induced regional warming in abrupt climate change during the last glacial period. Nature, 384(6608), 447-449.

Ram, M., Stolz, M., & Koenig, G. (1997). Late Holocene ice core records of dust and climate from the Greenland Ice Sheet. Journal of Geophysical Research: Atmospheres, 102(D22), 26333–26342

Ronneberger, O., Fischer, P., & Brox, T. (2015, October). U-net: Convolutional networks for biomedical image segmentation. In International Conference on Medical image computing and computer-assisted intervention (pp. 234-241). Cham: Springer international publishing.

Schaller, C. F., Freitag, J., & Eisen, O. (2017). Critical porosity of gas enclosure in polar firn independent of climate. Climate of the Past, 13(11), 1685-1693.

Spencer, M. K., Alley, R. B., & Fitzpatrick, J. J. (2006). Developing a bubble number-density paleoclimatic indicator for glacier ice. Journal of Glaciology, 52(178), 358-364.

Stoll, N., Eichler, J., Hörhold, M., Shigeyama, W., & Weikusat, I. (2021). A review of the microstructural location of impurities in polar ice and their impacts on deformation. Frontiers in Earth Science, 8, 615613.

Svensson, A., Baadsager, P., Persson, A., Hvidberg, C. S., & Siggaard - Andersen, M. L. (2003). Seasonal variability in ice crystal properties at NorthGRIP: a case study around 301 m depth. Annals of Glaciology, 37, 119-122.

Svensson, A., Nielsen, S. W., Kipfstuhl, S., Johnsen, S. J., Steffensen, J. P., Bigler, M., … & Röthlisberger, R. (2005). Visual stratigraphy of the North Greenland Ice Core Project (NorthGRIP) ice core during the last glacial period. Journal of Geophysical Research: Atmospheres, 110(D2), D02107.

Thompson, L. G., Yao, T., Davis, M. E., Henderson, K. A., Mosley-Thompson, E., Lin, P. -N., Beer, J., Synal, H. -A., Cole-Dai, J., & Bolzan, J. F. (1997). Tropicalclimate instability: The last glacial cycle from a Qinghai-Tibetan ice core. Science, 276(5320), 1821–1825.

Weikusat, I., Kipfstuhl, S., Faria, S. H., Azuma, N., & Miyamoto, A. (2009). Subgrain boundaries and related microstructural features in EDML (Antarctica) deep ice core. Journal of Glaciology, 55(191), 461-472.

Weikusat, I., Kuiper, E. J. N., Pennock, G. M., Kipfstuhl, S., & Drury, M. R. (2017). EBSD analysis of subgrain boundaries and dislocation slip systems in Antarctic and Greenland ice. Solid Earth, 8(5), 883-898.

https://doi.org/10.5194/egusphere-2025-4430
Preprint. Discussion started: 8 December 2025

Weiss, J., Vidot, J., Gay, M., Arnaud, L., Duval, P., & Petit, J. R. (2002). Dome Concordia ice microstructure: impurities effect on grain growth. Annals of Glaciology, 35, 552-558.

Yao, T., Thompson, L., & Yang, W. (2012). Different glacier status with atmospheric circulations in tibetan plateau and surroundings. Nature Climate Change, 2, 663-667.

Zhang, W., Huang, M., Xiang, C., & Azuma, K. (1993). A preliminary study of ice texture and fabric on an ice core to the bedrock extracted from Glacier No.1 at the headwater of Urumqi River, Tianshan, China. Bulletin of Glacier Research, (11), 9-15.